Polarization splitting of optical resonant modes in a-Si:H/a-SiO$_x$:H microcavities

A. A. Dukin,* N. A. Feoktistov, V. G. Golubev, A. V. Medvedev, A. B. Pevtsov, and A. V. Sel'kin
A. F. Ioffe Physico-Technical Institute, 26 Politechnicheskaya, St. Petersburg 194021, Russia
(Received 16 August 2002; published 8 April 2003)

We present experimental and theoretical results on polarization splitting of optical resonant modes in a-Si:H/a-SiO$_x$:H microcavities. It is shown experimentally that the splitting sign and value can be controlled by varying the active layer thickness. The polarization splitting achieved in the microcavities is about 8 meV owing to a large optical contrast, which is the ratio of film refractive indices in the distributed Bragg reflectors. The experimental data and theoretical analysis show that the polarization splitting may be zero at a certain angle of incidence of light determined by the microcavity parameters. The measured and calculated resonant frequency values for TM and TE polarizations were used to find the optical thickness of the active layer and the stop-band center frequency of the Bragg reflector. The account of the active layer thickness fluctuations along the lateral direction provides a better fit between the experimental and theoretical spectra.

DOI: 10.1103/PhysRevE.67.046602 PACS number(s): 42.55.Sa, 42.70.Qs, 42.25.Ja, 78.66.Jg

I. INTRODUCTION

Microcavities (MCs) composed of distributed Bragg reflectors (DBRs) and an active layer with a thickness of about the resonant wavelength have lately attracted much attention due to their unusual physical properties and promising applications in microelectronics [1]. In particular, MCs are widely used in light-emitting diodes to reduce radiation losses and in vertical cavity surface-emitting lasers to increase their efficiency and achieve a low threshold operation [2]. We have carried out a detailed study of the polarization characteristics of the optical (resonant) MC eigenmode. It is known that oblique light incidence produces a frequency difference in the resonant modes of TM and TE polarizations, which was first observed in MCs based on A^3B^5 semiconductors and termed polarization splitting [3]. The splitting in this MC type was found to be very small, less than the resonance line width. A more recent study [4] has shown that the polarization splitting in $Pb_{1-x}Eu_xTe/EuTe$ MCs with a high optical contrast (this is the ratio of the DBR layer refractive indices) is much larger than that in A^3B^5 MCs. This provides an additional degree of freedom for the MC radiation control [5].

The present work is aimed at a detailed investigation of polarization splitting in microcavities based on hydrogenated amorphous silicon (a-Si:H) and hydrogenated amorphous silicon-oxygen alloy (a-SiO$_x$:H). These materials possess a large ratio of refractive indices (the optical contrast is $n_{a\text{-Si:H}}/n_{a\text{-SiO}_x\text{:H}} \approx 2.4$ in the 1.3–1.5 μm range), which gives rise to a high splitting value. The MCs we studied were adjusted to the 1.3–1.5 μm wavelength range because it is commonly used in optical telecommunication systems. We will show that the splitting is closely related to the basic MC characteristics, providing additional information on the MC optical properties and design.

*Electronic address: dookin@gvg.ioffe.rssi.ru; URL: http://www.ioffe.ru/

II. EXPERIMENT

Polarization splitting was studied in MCs grown by the plasma-enhanced chemical vapor deposition (PECVD) technique. The cavities were planar structures, each consisting of a half-wave active layer placed between two DBRs. Each microcavity was grown in a single technological cycle without exposure to the air during the pauses between successive stages of growth of individual layers [6–9]. The a-Si:H films were deposited from a 10% silane-argon mixture. Up to 10% of oxygen was added to the gas mixture to deposit a-SiO$_x$:H films. The other PECVD parameters included the working pressure 0.1–0.2 Torr, RF power 0.03–0.1 W/cm^2, the substrate temperature 200 °C, and the gas flow rate 5–10 SCCM (SCCM denotes cubic centimeter per minute at STP). The average growth rate was less than 0.2 nm/s. *In situ* interferometry was used to control directly the film thickness, growth rate, and optical characteristics.

The film thicknesses were chosen such that the resonant wavelength of the eigenmode was within the range of 1.3–1.5 μm, a standard value for optical telecommunication systems. All of the MCs were made symmetric, i.e., the number of layers in the top and bottom DBRs was the same. We made MC structures with three and four layer pairs in DBRs.

One of the MC structures is shown schematically in Fig. 1. The top (A) and bottom (B) DBRs consist of three pairs (periods) of quarter-wave a-Si:H and a-SiO$_x$:H films $\lambda/4n_{a\text{-Si:H}}$ and $\lambda/4n_{a\text{-SiO}_x\text{:H}}$ thick and a half-wave a-Si:H active layer of thickness $\lambda/2n_{a\text{-Si:H}}$. Here, λ is the light wavelength in vacuum, $n_{a\text{-Si:H}}=3.46$, and $n_{a\text{-SiO}_x\text{:H}}=1.46$. The optical characteristics were found directly from the interference spectra during the growth. The characteristics of individual layers were controlled by ellipsometry independently. The MC structures had different active layer thicknesses which permitted obtaining different polarization splitting values. The quality factors (the ratio of the eigenmode resonance frequency to the eigenmode width) for structures with three periods (samples 222 and 340) and four periods (sample No. 342) were found to be 350, 470, and 950, respectively.

The reflection spectra for oblique incidence were mea-

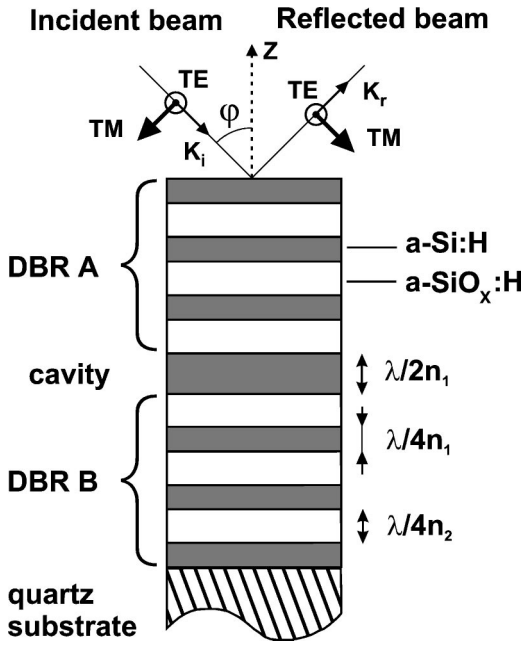

FIG. 1. Schematic diagram of a a-Si:H/a-SiO$_x$:H microcavity, consisting of a half-wave active layer placed between the top (A) and bottom (B) three-period distributed Bragg reflectors. TM and TE denote the polarization of light, φ is the angle of incidence of light, k_i and k_r are the wave vectors, n_1 and n_2 are the refractive indices.

sured by a computer-controlled diffraction grating monochromator equipped with a Hamamatsu InGaAs photodiode. The measurements were made in a lock-in mode regime. The surface area, which the reflected signal was detected from, was $100\times100\ \mu\text{m}^2$. The angular aperture was less than 1.5°, allowing us to avoid the undesirable broadening of the resonance lines because of the collection of rays that had passed through the structure at different angles.

The DBRs produce almost a total reflection band—a stop band. The MC reflectivity in the stop-band region is close to unity, and it is only the resonance frequency that produces a sharp dip associated with the resonant excitation of the MC

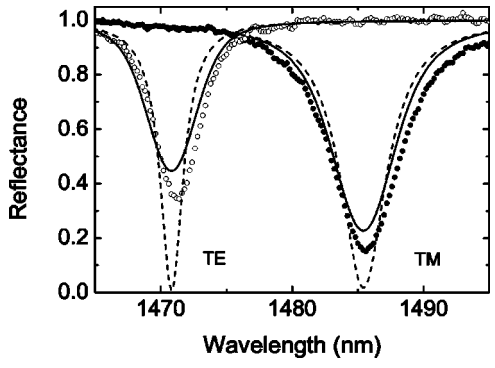

FIG. 2. Reflectance spectra of the a-Si:H/a-SiO$_x$:H microcavity with three-period DBRs, sample No. 222. The angle of incidence of light is 30°, TM and TE denote the polarization of light. Dotted lines are experimental data, solid and dashed lines are calculated with and without inhomogeneous broadening, respectively.

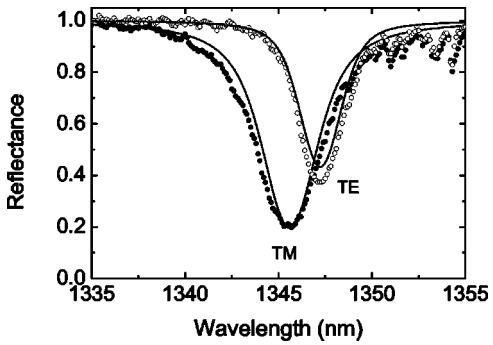

FIG. 3. Reflectance spectra of the a-Si:H/a-SiO$_x$:H microcavity with three-period DBRs, sample No. 340. The angle of incidence of light is 30°, TM and TE denote the polarization of light. Dotted lines are experimental data, solid lines represent calculations.

eigenmode. Figure 2 shows the reflection spectra for TM and TE polarizations in the region of resonance states of the MC eigenmodes (sample No. 222). The angle of incidence of light coming from the ambient (air) is 30°. One can see that the polarization splitting is larger than the total width of the resonance lines and that the lines have close amplitudes.

Figures 3 and 4 illustrate the spectra for samples 340 and 342 in the vicinity of the resonance lines of the eigenmodes. It is clearly seen that the polarization splitting value and sign vary with the sample due to the variation in the sample geometry (Table I). There is practically no splitting in sample No. 342 (Fig. 4).

III. THEORY

The frequency ω_r of the MC optical resonance mode can be found from the relation

$$\alpha_c\omega_r+\phi_A(\omega_r)+\phi_B(\omega_r)=2\pi N, \tag{1}$$

where $\phi_A(\omega_r)$ and $\phi_B(\omega_r)$ are the phase shifts of the electromagnetic wave reflected by the top (A) and bottom (B) DBRs at the resonance frequency; $\alpha_c(\varphi)=2L_c\text{Re}\,n_z/c$, $\alpha_c(\varphi)\omega_r$ is the phase increment on the doubled thickness $2L_c$ of the active layer; N is the integer, $n_z=\sqrt{\varepsilon_c-n_x^2}$, n_x

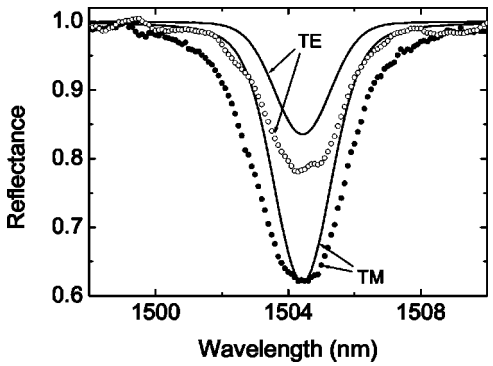

FIG. 4. Reflectance spectra of the a-Si:H/a-SiO$_x$:H microcavity with four-period DBRs, sample No. 342. The angle of incidence of light is 30°, TM and TE denote the polarization of light. Dotted lines are experimental data, solid lines represent calculations.

TABLE I. Microcavity characteristics found from the spectral analysis of polarization splitting and the resonance frequencies at the angle of incidence of 30°.

Sample No.	Fabry-Pérot frequency (meV)	Stop-band center frequency (meV)	TM-mode resonance frequency (meV)	TE-mode resonance frequency (meV)
222	958	733	834	842
340	891	898	921	920
342	803	788	824	824

$=\sqrt{\varepsilon_v}\sin\varphi$; φ is the light incidence angle; ε_c is the dielectric constant of the active layer; and ε_v is the dielectric constant of the ambient air. For simplicity, we will assume the amplitude (complex-valued) reflectivities r of both DBRs to be identical on the active layer side.

The energy reflectivity $R=|r|^2$ for the DBR in the stop-band region is practically frequency independent but the phase changes nearly linearly: $r^\sigma=\pm\sqrt{R^\sigma}\exp\{i\alpha^\sigma(\varphi)[\omega-\overline{\omega}^\sigma(\varphi)]\}$ [10], where σ is the TM or TE polarization, $\alpha^\sigma(\varphi)$ is the proportionality factor relating the phase to the frequency, $\overline{\omega}^\sigma(\varphi)$ is the frequency at the stop-band "center" (the phases 0 or π of the amplitude reflectivity) [11]. The phase shift of the wave reflected by DBR corresponds to the effective increase of the active layer thickness by the penetration depth, $\Delta L=\alpha(\varphi)c/2\,\mathrm{Re}\,n_z$, of the field into the DBR. The coefficient α is inversely proportional to the difference in the refractive indices: $\alpha(0)=\overline{\lambda}n_1n_2/[2c(n_1-n_2)\sqrt{\varepsilon_c}]$, where n_1 and n_2 are the refractive indices of the DBR films ($n_1>n_2$), $\overline{\lambda}=2\pi c/\overline{\omega}(0)$, and $\overline{\omega}(0)\equiv\overline{\omega}^{\mathrm{TM}}(0)=\overline{\omega}^{\mathrm{TE}}(0)$ [12]. The phase of the amplitude reflectivity at the frequency $\overline{\omega}^\sigma(\varphi)$ is zero, if the active layer has a high refractive index $\sqrt{\varepsilon_c}=n_1$, like in our case, or it is equal to π, if the active layer has a lower refractive index $\sqrt{\varepsilon_c}=n_2$.

The phase dependences of the amplitude reflectivities for the top and bottom DBRs may differ. In that case, one should express $\alpha^\sigma(\varphi)$ and $\overline{\omega}^\sigma(\varphi)$ as

$$\alpha^\sigma(\varphi)=[\alpha_A^\sigma(\varphi)+\alpha_B^\sigma(\varphi)]/2$$

and

$$\overline{\omega}^\sigma(\varphi)=[\alpha_A^\sigma(\varphi)\overline{\omega}_A^\sigma(\varphi)+\alpha_B^\sigma(\varphi)\overline{\omega}_B^\sigma(\varphi)]/[\alpha_A^\sigma(\varphi)+\alpha_B^\sigma(\varphi)],$$

where $\alpha_A^\sigma(\varphi)$ and $\alpha_B^\sigma(\varphi)$ are the proportionality factors for the A and B reflectors, respectively; $\overline{\omega}_A^\sigma(\varphi)$ and $\overline{\omega}_B^\sigma(\varphi)$ are the stop-band center frequencies for the A and B DBRs, respectively.

With increasing incidence, the coefficient α becomes larger for the TM polarization but it is smaller for the TE polarization; the position of the stop-band center also varies with the polarization. According to the Fresnel formulas, this is due to the respective changes in the TM and TE reflectivities at the layer interfaces in the DBR. As a result, the resonance conditions (1) for the TM and TE polarizations become different, producing the polarization splitting: the mode resonance frequencies $\omega_r^{\mathrm{TM}}(\varphi)$ and $\omega_r^{\mathrm{TE}}(\varphi)$ differ. For the definite polarization σ, we have

$$\omega_r^\sigma(\varphi)=\frac{2\pi N+2\alpha^\sigma(\varphi)\overline{\omega}^\sigma(\varphi)}{\alpha_c(\varphi)+2\alpha^\sigma(\varphi)}, \tag{2}$$

where $\alpha_c(\varphi)\equiv 2\pi N/\omega_{FP}(\varphi)$, $\omega_{FP}(\varphi)\equiv\omega_{FP}(0)\mathrm{Re}\sqrt{\varepsilon_c}/\mathrm{Re}\,n_z$, and $\omega_{FP}(0)\equiv\pi cN/L_c\,\mathrm{Re}\sqrt{\varepsilon_c}$ is the MC eigenmode frequency at normal incidence if there are no phase shifts of the waves reflected by DBRs (the Fabry-Pérot frequency [10]).

Using Eq. (2), one can show that the polarization splitting is proportional to the difference in the frequencies $\omega_{FP}(0)$ and $\overline{\omega}(0)$:

$$\omega_r^{\mathrm{TM}}(\varphi)-\omega_r^{\mathrm{TE}}(\varphi)=A(\varphi)[\omega_{FP}(0)-\overline{\omega}(0)]+B(\varphi), \tag{3}$$

where

$$A(\varphi)=-\frac{2\alpha_c(\varphi)[\alpha^{\mathrm{TM}}(\varphi)-\alpha^{\mathrm{TE}}(\varphi)]\mathrm{Re}\sqrt{\varepsilon_c}}{[\alpha_c(\varphi)+2\alpha^{\mathrm{TM}}(\varphi)][\alpha_c(\varphi)+2\alpha^{\mathrm{TE}}(\varphi)]\mathrm{Re}\,n_z}, \tag{4}$$

$$B(\varphi)=\frac{2\alpha_c(\varphi)[\alpha^{\mathrm{TM}}(\varphi)-\alpha^{\mathrm{TE}}(\varphi)]\overline{\omega}(0)}{[\alpha_c(\varphi)+2\alpha^{\mathrm{TM}}(\varphi)][\alpha_c(\varphi)+2\alpha^{\mathrm{TE}}(\varphi)]}\left(\frac{\overline{\omega}^{\mathrm{TM}}(\varphi)}{\overline{\omega}(0)}-\frac{\omega_{FP}(\varphi)}{\omega_{FP}(0)}\right)+\frac{2\alpha^{\mathrm{TE}}(\varphi)[\overline{\omega}^{\mathrm{TM}}(\varphi)-\overline{\omega}^{\mathrm{TE}}(\varphi)]}{\alpha_c(\varphi)+2\alpha^{\mathrm{TE}}(\varphi)}. \tag{5}$$

Equation (3) holds on the assumption of a linear frequency dependence of the reflectivity phase. The polarization splitting is primarily due to the difference in the $\alpha^\sigma(\varphi)$ coefficients for the TM and TE polarizations. The difference $\alpha^{\mathrm{TM}}(\varphi)-\alpha^{\mathrm{TE}}(\varphi)$ enters into expression (4) and into the first term of Eq. (5). Besides, contributions to the polarization splitting are also made by the difference in the stop-band center frequencies, $\overline{\omega}^{\mathrm{TM}}(\varphi)-\overline{\omega}^{\mathrm{TE}}(\varphi)$ [the second term in Eq. (5)], and by the different angular dependences of the Fabry-Pérot frequency $\omega_{FP}(\varphi)$ and the stop-band center frequency $\overline{\omega}^\sigma(\varphi)$ [the first term in Eq. (5)].

At normal incidence, the polarization splitting is zero, $A(0)=0$ and $B(0)=0$, since the waves with different polarizations are then reflected similarly, $\alpha^{\mathrm{TM}}(0)=\alpha^{\mathrm{TE}}(0)$ and $\overline{\omega}^{\mathrm{TM}}(0)=\overline{\omega}^{\mathrm{TE}}(0)$. As the incidence angle becomes larger, the polarization splitting rises superlinearly because of the nonlinear growth of the difference $\alpha^{\mathrm{TM}}(\varphi)-\alpha^{\mathrm{TE}}(\varphi)$.

The polarization splitting equals $B(\varphi)$ in "optimal" MC structures when $\omega_{FP}(0)=\overline{\omega}(0)$. The calculated value of the relative splitting

$$\Delta_{\mathrm{TM,TE}}\equiv 2[\omega_r^{\mathrm{TM}}(\varphi)-\omega_r^{\mathrm{TE}}(\varphi)]/[\omega_r^{\mathrm{TM}}(\varphi)+\omega_r^{\mathrm{TE}}(\varphi)]$$

in the a-Si:H/a-SiO$_x$:H structures is 10^{-3} at the incidence of 30°. This is in good agreement with the theoretical resonance line width in structures of the three-period DBRs, indicating the possibility of experimental observation of the

splitting. The splitting value can be increased manifold owing to the mismatch between the frequencies $\omega_{FP}(0)$ and $\overline{\omega}(0)$. The polarization splitting sign is governed by the sign of the difference $\omega_{FP}(0)-\overline{\omega}(0)$.

It follows directly from Eq. (3) that we can select such values of $\omega_{FP}(0)$ and $\overline{\omega}(0)$ that the splitting will vanish at a certain angle of incidence. The angular dependence of the polarization splitting will then become nonmonotonous. The reason for zero splitting at oblique incidence is that the phase shift of the light wave reflected by the DBR is the same for both polarizations at the resonance frequency [Eq. (1)]. The condition for zero splitting then takes the form

$$L_c=\frac{[\alpha^{\mathrm{TM}}(\varphi)-\alpha^{\mathrm{TE}}(\varphi)]2\pi N+2\alpha^{\mathrm{TM}}(\varphi)\alpha^{\mathrm{TE}}(\varphi)[\overline{\omega}^{\mathrm{TE}}(\varphi)-\overline{\omega}^{\mathrm{TM}}(\varphi)]}{\alpha^{\mathrm{TM}}(\varphi)\overline{\omega}^{\mathrm{TM}}(\varphi)-\alpha^{\mathrm{TE}}(\varphi)\overline{\omega}^{\mathrm{TE}}(\varphi)}\frac{c}{2\,\mathrm{Re}\,n_z}.$$

In this case, the phase difference between the TM and TE waves reflected by the MC structure is nonzero, in contrast to the normal incidence. Therefore, the linearly polarized light containing the TM and TE components becomes elliptically polarized. The parameters of the polarization ellipse vary greatly within the resonant contour.

Note that the value of $\Delta_{\mathrm{TM,TE}}$ for conventional GaAs/AlAs structures is less than 0.1% at 60° incidence [10] because of the low optical contrast in A^3B^5 DBRs [2]. The polarization splitting can be increased by using high index contrast DBRs [4]. In particular, the splitting can be made an order of magnitude larger by using higher optic contrast: at low contrast $\alpha^{\mathrm{TM}},\alpha^{\mathrm{TE}}\gg\alpha_c$, whereas at high contrast $\alpha^{\mathrm{TM}},\alpha^{\mathrm{TE}}\sim\alpha_c$ [see Eqs. (4) and (5)].

IV. RESULTS AND DISCUSSION

A. Polarization splitting of the optical resonant mode

The MC reflection spectra were calculated using Airy's formulas [13]. The theoretical resonance frequencies were fitted to the experimental ones by varying two parameters—the active layer thickness L_c and the frequency $\overline{\omega}(0)$—and taking the above values of the MC refractive indices. The theoretical spectra were computed taking into account the inhomogeneous broadening of the resonant contour (see below).

It is found that sample No. 222 has a higher resonance frequency for the TE polarization than for the TM polarization (Fig. 2), whereas the optimal MC structure shows the contrary result. The latter is due to the fact that the Fabry-Pérot frequency $\omega_{FP}(0)$ for sample No. 222 is higher than its stop-band center frequency $\overline{\omega}(0)$.

Figure 3 illustrates the polarization splitting for sample No. 340 at the same incidence of 30°, which shows the reverse sequence of the TM and TE components, as compared with sample No. 222. The lower value of polarization splitting results from the smaller difference between the frequencies $\omega_{FP}(0)$ and $\overline{\omega}(0)$, with the opposite splitting sign being due to the condition $\omega_{FP}(0)<\overline{\omega}(0)$.

Therefore, the polarization splitting can be controlled by varying the active layer thickness, and zero splitting can be achieved by selecting the proper angle of incidence (Fig. 4).

The values of $\omega_{FP}(0)$ and $\overline{\omega}(0)$ were found by fitting the theoretical TM and TE resonance frequencies (Table I).

The polarization splitting is practically independent on the number of layers in the DBR but it increases with larger difference $\omega_{FP}(0)-\overline{\omega}(0)$ or higher optical contrast. The overlap of the resonance lines can be reduced by making the lines narrower by increasing the number of layers in the DBRs.

Figure 5 shows the calculated polarization splitting $\Delta_{\mathrm{TM,TE}}$ at the light incidence of 30° as a function of the relative mismatch $\Delta_{FP}\equiv[\omega_{FP}(0)-\overline{\omega}(0)]/\overline{\omega}(0)$ between the Fabry-Pérot and stop-band center frequencies (solid line). The splitting varies nearly linearly with the difference $\omega_{FP}(0)-\overline{\omega}(0)$. Sample No. 340 is closest to the optimal MC structure. The comparison of the spectra for samples 340 and 222 shows that the splitting can be increased by an order of magnitude by changing the value of Δ_{FP} from 0 to 0.3. Sample No. 342 shows no splitting at the light incidence of 30° (Fig. 5). The inset in Fig. 5 gives the theoretical values of the relative polarization splitting $\Delta_{\mathrm{TM,TE}}$ for this sample as a function of the angle of incidence φ. One can see that this

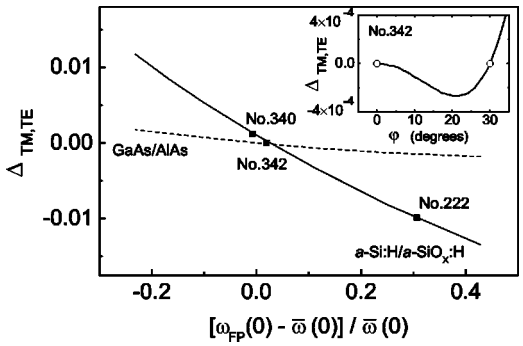

FIG. 5. Relative polarization splitting, $\Delta_{\mathrm{TM,TE}}$, as a function of relative mismatch, $[\omega_{FP}(0)-\overline{\omega}(0)]/\overline{\omega}(0)$, between the Fabry-Pérot frequency and the stop-band center frequency of DBRs. The solid line is calculated for a-Si:H/a-SiO_x:H microcavities, squares are the experimental data for a-Si:H/a-SiO_x:H microcavities, and the dashed line represents calculation for GaAs/AlAs microcavities. Inset: calculated angular dependence of the relative polarization splitting for the a-Si:H/a-SiO_x:H microcavity, sample No. 342. Indicated by open circles are zeros of the splitting.

splitting vanishes and reverses its sign at the 30° incidence. So, $\Delta_{\mathrm{TM,TE}}$ equals zero at two angles of incidence, $\varphi=0°$ and $\varphi=30°$, that are pointed in the inset by open circles. Unfortunately, our samples under study do not permit measuring the nonmonotonic part of the curve $\Delta_{\mathrm{TM,TE}}(\varphi)$ due to the experimental error in determining difference in spectral positions of reflectivity minima. Only at the angle of $\varphi=40°$ and higher, the polarization splitting becomes measurable for the sample No. 342.

Figure 5 also presents the theoretical dependence of $\Delta_{\mathrm{TM,TE}}$ on Δ_{FP} for GaAs/AlAs MC structures of low optical contrast ($n_{\mathrm{GaAs}}=3.55$ and $n_{\mathrm{AlAs}}=3.01$ at the wavelength $\lambda=886$ nm [14]). It is evident that the value of $\Delta_{\mathrm{TM,TE}}$ for a-Si:H/a-SiO_x:H structures is nearly an order of magnitude larger than that for GaAs/AlAs structures.

The approximate dependence of polarization splitting on $\omega_{FP}(0)-\overline{\omega}(0)$ was pointed out earlier [10]. As compared with the corresponding formulas of Ref. [10], our formula (3) contains an additional term B, besides the analytical expression for the term A is different from that for analogous term in Ref. [10]. Therefore our formula is valid for both high and low optical contrasts, whereas the formulas of Ref. [10] are limited only by the case of low optical contrast.

In the case of low optical contrast [and a reasonable difference $\omega_{FP}(0)-\overline{\omega}(0)$], we have $|B(\varphi)|\ll|A(\varphi)[\omega_{FP}(0)-\overline{\omega}(0)]|$. Then the polarization splitting is close to zero at any angle of incidence when $\omega_{FP}(0)=\overline{\omega}(0)$. At $\omega_{FP}(0)\neq\overline{\omega}(0)$, however, the splitting may be appreciable as its absolute value increases monotonically with the incidence angle. At high contrast, the $|B(\varphi)|/|A(\varphi)[\omega_{FP}(0)-\overline{\omega}(0)]|$ ratio becomes an order of magnitude larger, such that the $B(\varphi)$ factor should not be ignored anymore. The latter leads to the splitting that will occur even at $\omega_{FP}(0)=\overline{\omega}(0)$. Zero splitting can be achieved by the proper selection of the values $\omega_{FP}(0)\neq\overline{\omega}(0)$ and the angle of incidence φ. Then the splitting angular dependence becomes nonmonotonous (for the calculations, see the inset in Fig. 5).

The angular dependences of the resonance frequencies for the TM- and TE-polarizations are presented in Fig. 6 for sample No. 222 having a large value of $\Delta_{\mathrm{TM,TE}}$. The splitting grows nonlinearly as the angle of incidence becomes larger. The inset shows the MC reflectivities for the TM and TE polarizations, calculated taking into account the inhomogeneous broadening, as a function of the angle of incidence at the fixed light wavelength of 1.44 μm. The angles, at which resonant modes are excited at this wavelength, differ by a few degrees. The experimental points and theoretical curves in Fig. 6 demonstrate mode states of different energies, wave vectors, and polarizations. Some of the states are energy degenerate but have different wave vectors and polarizations. This is illustrated in the inset of Fig. 6 for two degenerate states.

It is noteworthy that the calculation of the MC quality factor must consider the spectral variation of the DBR reflectivity phase. For this case, the theoretical quality factor is defined as [15] $Q=\omega_r(0)/\Gamma=\sqrt{R}[\alpha_c(0)+2\alpha(0)]\omega_r(0)/2(1-R)$, where Γ is the resonance line width in the reflection or transmission spectrum at normal incidence. The quality factor increases by a factor of $1+2\alpha(0)/\alpha_c(0)$ because of the phase shift in the DBR reflection. With the spectral dependence of the phase, the theoretical value of this parameter appears to be 1.7 times higher in a-Si:H/a-SiO_x:H structures.

The detuning between $\omega_{FP}(0)$ and $\overline{\omega}(0)$ leads not only to a larger polarization splitting but to a smaller quality factor. Figure 7 presents the quality factor calculations for a-Si:H/a-SiO_x:H MC structures with three-period DBRs as a function of the detuning Δ_{FP} (solid line). The inhomogeneous broadening was ignored. It is seen that the quality factor decreases with increasing the absolute value of Δ_{FP}. This is due to the fact that the reflectivity reaches a maximum in the vicinity of the stop-band center and then smoothly decreases towards the stop-band edges. Owing to the increase in Δ_{FP} from 0 to 0.3, the splitting grows by an order of magnitude (sample No. 222 in Fig. 5) but quality factor drops 1.6 times. A comparison with the experimental quality factors for a-Si:H/a-SiO_x:H samples of three-period DBRs and different values of Δ_{FP} and $\overline{\omega}(0)$ (indicated by circles) shows that they depend on Δ_{FP} to a lesser degree. Besides, the experimental values are smaller than the theoretical ones, which we attribute to the inhomogeneous broadening of the resonance lines.

B. Inhomogeneous broadening of resonance lines

The above approach to the calculation of reflection spectra fails to provide a complete agreement with the experimental data. The calculated and measured resonance frequencies coincide, but the theoretical resonance line widths appear to be smaller and the amplitudes larger than the experimental values. A possible reason for this discrepancy is the inhomogeneous broadening of the reflection line, associated with active layer thickness fluctuations within the sample lateral area which makes a contribution to the registered signal. Another possible mechanism of the broadening could occur, in principle, due to fluctuations of the susceptibility (see, for example, Ref. [16]). However, in the microcavities investigated, the layer susceptibilities have no resonant peculiarities. Therefore such kind of a broadening mechanism seems unlikely in our case. On the other hand, rather small random deviations ($\delta L_c\approx 0.2-0.4$ nm) of the active layer thickness ($L_c\approx 200$ nm) bring about a remarkable shift ($\approx 0.6-1.2$ nm) of the eigenmode wavelength, which allows one to give a simple explanation for the observed broadening of the reflection lines.

Figure 2 shows the resonance lines of the reflection spectra for sample No. 222; solid and dashed lines are calculated with and without the inhomogenous broadening, respectively, assuming the Gaussian distribution of the active layer thicknesses and performing an averaging of the reflectivity. The broadening decreases the amplitude of the TE line as compared with the TM line, increasing the widths of both lines. However, the position of the minimum and the contour area remain the same. Therefore, the inhomogeneous broadening does not affect the polarization splitting but makes the spectral line overlap larger.

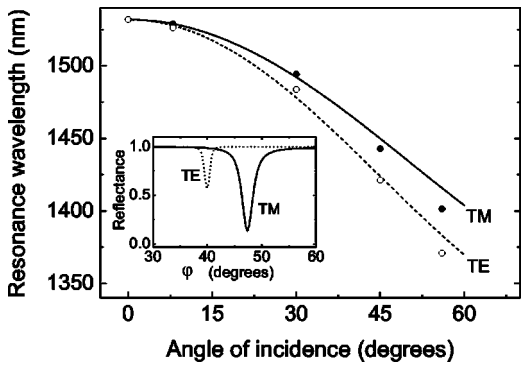

FIG. 6. Angular dependences of the resonance frequencies for a-Si:H/a-SiO_x:H microcavity with three-period DBRs, sample No. 222. TM and TE denote the polarization of light. Solid and dashed lines—calculation, circles—the experimental data. Inset: the a-Si:H/a-SiO_x:H microcavity (sample No. 222) reflectance as a function of the angle of incidence at the fixed wavelength of 1.44 μm.

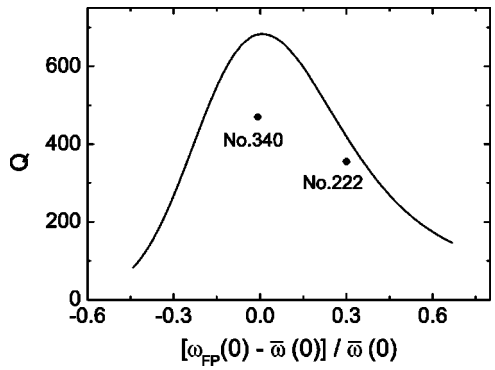

FIG. 7. Quality factor, $Q=\omega_r(0)/\Gamma$, as a function of relative mismatch, $[\omega_{FP}(0)-\bar{\omega}(0)]/\bar{\omega}(0)$, between the Fabry-Pérot and the stop-band center frequencies for a-Si:H/a-SiO_x:H microcavities with three-period DBRs. Solid line—calculation, circles—the experimental data.

The account of thickness fluctuations provides a better fitting of the theoretical spectra. The mean square deviation of the active layer thickness is found to be 0.4 nm for sample No. 222 (Fig. 2) and 0.2 nm for samples 340 (Fig. 3) and 342 (Fig. 4). It is the resonance character of this effect that allows a spectroscopic registration (from the line amplitude and width) of the thickness fluctuations, which are as small as a few angstroms. A high sensitivity to such minute fluctuations was reported earlier in the analysis of the elastic resonant light scattering on the interface roughness in a MC structure with a quantum well in the active layer [17].

The theoretical line widths for sample No. 222 (Fig. 2) are close to the experimental width values but the amplitudes appear to be somewhat lower. The latter may be due to a lower DBR reflectivity because of the thickness deviation from the quarter-wave value [15].

Thus, the suggested mechanism of inhomogeneous broadening of the resonance lines provides a better agreement between theoretical and experimental reflection spectra. The discrepancy between the model calculations and experimental data for sample No. 342 seems to be due to a smaller line width in this sample (with four-period DBRs) than in samples 222 and 340 (with three-period DBRs). A smaller width makes the line more sensitive to additional broadening factors that were not included in the model.

V. CONCLUSION

Plasma-enhanced chemical vapor deposition was used to make a series of planar a-Si:H/a-SiO_x:H based microcavities with different geometry parameters. The experimental and theoretical investigation of optical resonant modes in these structures has shown that their polarization splitting is an order of magnitude larger than in conventional A^3B^5 microcavities owing to a large interface optical contrast in the distributed Bragg reflectors. The focus was on the variation of the polarization splitting of resonant lines in the light reflection spectra with the microcavity parameters and the angle of light incidence. It is shown experimentally that the sign of splitting and its value essentially depend on the active layer thickness. The high optical contrast provides about 1% relative splitting at the incidence of 30°. We have studied experimentally and theoretically the conditions under which energy-degenerate TE- and TM-mode states can be excited at zero splitting. The active layer thickness and the stop-band center frequency in distributed Bragg reflectors were found by fitting the calculated resonance frequencies for the TM and TE modes to their experimental values.

The detailed analysis of the resonant reflection lines indicates the presence of statistical roughnesses at the film interfaces, which produce fluctuations in the active layer thickness. The account of such fluctuations in the model calculations allowed the evaluation of the mean square deviation of the thickness, which was found to be only a few angstroms. It is the resonant character of the light reflection effect in the region of eigenmode states that makes possible a spectroscopic registration of such minute thickness fluctuations from the resonant line amplitude and width.

ACKNOWLEDGMENTS

This work was supported by the RFBR under Grant No. 02-02-17601 and the program of the Russian Ministry of Science and Technologies ''Physics of Solid State Nanostructures.''

[1] J. Rarity and C. Weisbuch, *Microcavities and Photonic Bandgaps: Physics and Applications* (Kluwer, Dordrecht, 1996).

[2] A. Miller, M. Ebrahimzadeh, and D. M. Finlayson, *Semiconductor Quantum Optoelectronics: From Quantum Physics to Smart Devices* (Institute of Physics Publishing, Bristol, 1999).

[3] D. Baxter, M.S. Skolnick, A. Armitage, V.N. Astratov, D.M. Whittaker, T.A. Fisher, J.S. Roberts, D.J. Mowbray, and M.A. Kaliteevski, Phys. Rev. B **56**, R10 032 (1997).

[4] W. Heiss, T. Schwarzl, and G. Springholz, Phys. Status Solidi A **188**, 929 (2001).
[5] T. Virgili, D.G. Lidzey, D.D.C. Bradley, and S. Walker, Synth. Met. **116**, 497 (2001).
[6] A.B. Pevtsov, A.V. Zherzdev, N.A. Feoktistov, G. Juska, T. Muschik, and R. Schwarz, Int. J. Electron. **78**, 289 (1995).
[7] N.A. Feoktistov, N.L. Ivanova, L.E. Morozova, Yu.A. Nikulin, A.P. Onokhov, A.B. Pevtsov, and R. Schwarz, in *Amorphous Silicon Technology—1996*, edited by M. Hack, E. A. Schiff, S. Wagner, A. Matsuda, and R. Schropp, MRS Symposia Proceedings No. 420 (Materials Research Society, Pittsburgh, 1996), p. 189.
[8] A.A. Dukin, N.A. Feoktistov, V.G. Golubev, A.V. Medvedev, A.B. Pevtsov, and A.V. Sel'kin, Appl. Phys. Lett. **77**, 3009 (2000).
[9] A.A. Dukin, N.A. Feoktistov, V.G. Golubev, A.V. Medvedev, A.B. Pevtsov, and A.V. Sel'kin, J. Non-Cryst. Solids **299-302**, 694 (2002).
[10] G. Panzarini, L.C. Andreani, A. Armitage, D. Baxter, M.S. Skolnick, V.N. Astratov, J.S. Roberts, A.V. Kavokin, M.R. Vladimirova, and M.A. Kaliteevski, Phys. Rev. B **59**, 5082 (1999); Phys. Solid State **41**, 1223 (1999).
[11] Calculations show that this frequency lies approximately at the center of the actual stop band if the DBR has a sufficiently large number of periods and there is no absorption.
[12] R. Ram, D. Babic, R. York, and J. Bowers, IEEE J. Quantum Electron. **31**, 399 (1995).
[13] A. Yariv and P. Yeh, *Optical Waves in Crystals* (Wiley, New York, 1984).
[14] J.T. Boyd, IEEE J. Quantum Electron. **8**, 788 (1972).
[15] V.G. Golubev, A.A. Dukin, A.V. Medvedev, A.B. Pevtsov, A.V. Sel'kin, and N.A. Feoktistov, Semiconductors **35**, 1213 (2001).
[16] V. Savona, S. Haacke, and B. Deveaud, Phys. Rev. Lett. **84**, 183 (2000).
[17] V.A. Kosobukin and A.V. Sel'kin, Phys. Solid State **42**, 1914 (2000).